Precision-Cut Kidney Slices as a Tool to Understand the Dynamics of Extracellular Matrix Remodeling in Renal Fibrosis

Federica Genovese, Zsolt S. Kàrpàti, Signe H. Nielsen and Morten A. Karsdal

Nordic Bioscience, Herlev, Denmark.

ABSTRACT: The aim of this study was to set up an *ex vivo* model for renal interstitial fibrosis in order to investigate the extracellular matrix (ECM) turnover profile in the fibrotic kidney. We induced kidney fibrosis in fourteen 12-week-old male Sprague Dawley rats by unilateral ureteral obstruction (UUO) surgery of the right ureter. The left kidney (contralateral) was used as internal control. Six rats were sham operated and used as the control group. Rats were terminated two weeks after the surgery; the kidneys were excised and precision-cut kidney slices (PCKSs) were cultured for five days in serum-free medium. Markers of collagen type I formation (P1NP), collagen type I and III degradation (C1M and C3M), and α-smooth muscle actin (αSMA) were measured in the PCKS supernatants by enzyme-linked immunosorbent assay. P1NP, C1M, C3M, and α-SMA were increased up to 2- to 13-fold in supernatants of tissue slices from the UUO-ligated kidneys compared with the contralateral kidneys ($P < 0.001$) and with the kidneys of sham-operated animals ($P < 0.0001$). The markers could also reflect the level of fibrosis in different animals. The UUO PCKS *ex vivo* model provides a valuable translational tool for investigating the extracellular matrix remodeling associated with renal interstitial fibrosis.

KEYWORDS: PCKS, *ex vivo*, kidney fibrosis, UUO, extracellular matrix

CITATION: Genovese et al. Precision-Cut Kidney Slices as a Tool to Understand the Dynamics of Extracellular Matrix Remodeling in Renal Fibrosis. *Biomarker Insights* 2016:11 77–84 doi: 10.4137/BMI.S38439.

TYPE: Original Research

RECEIVED: January 07, 2016. **RESUBMITTED:** March 01, 2016. **ACCEPTED FOR PUBLICATION:** March 05, 2016.

ACADEMIC EDITOR: Karen Pulford, Editor in Chief

PEER REVIEW: Four peer reviewers contributed to the peer review report. Reviewers' reports totaled 1,476 words, excluding any confidential comments to the academic editor.

FUNDING: This work was funded by "Den Danske Forskningsfond". The authors confirm that the funder had no influence over the study design, content of the article, or selection of this journal.

COMPETING INTERESTS: FG, SHN, and MAK are full-time employees of Nordic Bioscience A/S. Nordic Bioscience is a privately owned, small-medium size enterprise (SME) partly focused on the development of biomarkers. None of the authors received fees, bonuses, or other benefits for the work described in the manuscript. MAK holds stocks in Nordic Bioscience A/S.

CORRESPONDENCE: fge@nordicbioscience.com

Paper subject to independent expert blind peer review. All editorial decisions made by independent academic editor. Upon submission manuscript was subject to anti-plagiarism scanning. Prior to publication all authors have given signed confirmation of agreement to article publication and compliance with all applicable ethical and legal requirements, including the accuracy of author and contributor information, disclosure of competing interests and funding sources, compliance with ethical requirements relating to human and animal study participants, and compliance with any copyright requirements of third parties. This journal is a member of the Committee on Publication Ethics (COPE). Provenance: the authors were invited to submit this paper.

Published by Libertas Academica. Learn more about this journal.

Introduction

Fibrotic diseases are responsible for 45% of deaths in the Western world[1]; renal fibrosis is a common hallmark of chronic kidney disease[2] and is the best predictor of progression to end-stage renal disease.[3] Despite the extensive research focusing on finding new drug candidates to stop or reverse the fibrotic process, there are at present no efficacious treatments for renal fibrosis.[4] Understanding the mechanisms involved in the development of fibrosis is important to identify specific pharmacological targets, but the ability to monitor the dynamic process of excessive remodeling of the extracellular matrix (ECM) in real time is also of equal importance, which is fundamental in the selection process of candidate drugs. There is currently a need for noninvasive soluble biomarkers that can monitor this dynamic turnover and potentially change as a consequence of antifibrotic treatment. Such biomarkers could aid in translational research to translate the results obtained in *ex vivo* and *in vivo* systems to clinical settings. Fibrosis is a disease of the matrix; therefore, to understand the pathology of the disease, it is important to understand the fluctuation of the ECM turnover, in which both tissue formation and tissue degradation are upregulated.[5,6] This complex system, which involves many different cell types and inflammatory molecules and proteases, cannot be fully understood in cell-based *in vitro* models.[7] Precision-cut tissue slices (PCTSs) can represent a valid alternative to *in vivo* experiments to study the mechanism and efficacy of antifibrotic drug candidates, since they are cost-effective in terms of number of animals needed for the experiments[8] and are more representative of the complex cell–cell and cell–matrix cross-talk than *in vitro* cultures of fibroblasts.[7] In fact, the main difference between this system and cell-based *in vitro* settings is the presence of the matrix in its natural conformation. Therefore, this system allows for the monitoring of the modifications of the matrix in pathological conditions, ie, the formation and degradation of ECM proteins during fibrosis.

The use of PCTSs to investigate the mechanisms of fibrosis has flourished in the past few years,[9] and it has been successful in elucidating certain mechanisms involved in fibrosis onset and progression.[4] In literature, the unilateral ureteral obstruction (UUO) model in rats[10] and high-NaCl-fed DDR1 null mice[4] have been previously used as source of tissue for

precision-cut kidney slice (PCKS) to study the mechanisms of chronic kidney disease. However, the cultures were carried out for a short time (45 minutes) on 1.5 mm thick slices,[8] since the scope of the experiment was mainly to observe fast pharmacodynamics.[10]

In this work, we developed an *ex vivo* model of PCKS using fibrotic kidneys from UUO-operated rats. We cultured the slices for five days in order to observe the dysregulated ECM remodeling in a chronic system. We measured soluble fragments of ECM proteins that were released into the supernatant of the tissue cultures in order to identify the protein fingerprint of the disease and to find suitable biomarkers for future applications in drug discovery and selection.

Materials and Methods

Unilateral ureteral obstruction. Twenty 12-week-old male Sprague Dawley rats (Harlan) were used in this experiment. The rats were kept two per cage in standard type III–H cages with standard bedding (Tapvei Oy) and nest material (Tapvei Oy), both changed twice a week. They were fed with standard pellet diet (24% protein, 11% fat, and 65% carbohydrates, Altromin International) and tap water ad libitum and kept under 12-hour dark/light cycles at 20 °C ± 2 °C with a relative humidity of 50% ± 20%. The animals were divided into two groups: 6 animals underwent sham surgery, while 14 rats underwent UUO. Rats were anesthetized with 5% and then 3% isoflourane by inhalation and with 20 mg lidocaine by intradermal injection. A 6- to 9-cm-long surgical cut was performed in the midline of the abdomen, and the right ureter was ligated with a nonabsorbable suture, 3–4 cm down the renal pelvis. The sham-operated control rats underwent only the surgical cut of the abdomen and peritoneum followed by closure.

At 14 days after surgery, the rats were anesthetized with 5% and then 3% isoflourane by inhalation and terminated by a throat and spine cut. The kidneys were then excised and stored in oxygen-enriched freshly prepared ice-cold Krebs–Henseleit buffer (2.5 mM $CaCl_2$, 5 mM KCl, 118 mM NaCl, 1.1 mM $MgSO_4$, and 1.2 mM KH_2PO_4) supplemented with 25 mM glucose, 10 mM HEPES, and 25 mM $NaHCO_3$ until further use.

This study was approved by the Experimental Animal Committee of the Danish Ministry of Justice (approval number 2012-DY-2934-00003).

Precision-cut tissue slices. The collected kidneys were washed in Krebs–Henseleit buffer, the perinephric fat was eliminated, and the kidneys were cut on the sagittal plane. One half was transferred into a tube containing 4% formaldehyde for fixation. After 24 hours, the specimens were transferred into 0.4% formaldehyde and embedded in paraffin using the Sakura Tissue-Tek VIP6 tissue embedder according to manufacturer's instructions.

Three 8 mm diameter biopsy punches were cut from the remaining half of the kidney, maximizing the content of renal cortex and medulla over renal pelvis, and were transferred to a TSE Systems Krumdieck Tissue Slicer MD4000, containing 1 L ice-cold Krebs–Henseleit buffer. Twelve standardized slices (250 µm thickness, 15 ± 3 mg, dry weight) representative of the three punches were cut from each kidney of each animal and then transferred to a 48-well tissue culture plate in 400 µL William's E + GlutaMAX medium (Sigma-Aldrich) supplemented with 1:100 D(+)Glucose (Sigma-Aldrich), 1:50 penicillin/streptomycin mix (Sigma-Aldrich), and 1:200 antifungal solution. The plates were cultured for 5 days at 37 °C at 150 rpm, in a 95% O_2/5% CO_2 atmosphere. Tissue viability was examined by diluting AlamarBlue® (Life Technologies) in culture medium (10×), which was preheated at 37 °C. The diluted AlamarBlue® mix was added to the tissue cultures. After 1 hour incubation at 37 °C, 150 rpm in 95% O_2/5% CO_2 atmosphere, fluorescence in the supernatants was measured on an enzyme-linked immunosorbent assay (ELISA) reader using 540 nm as excitation wavelength and 590 nm as emission wavelength. Wells containing just AlamarBlue® were used as background control, and their fluorescence value was subtracted from the sample values.

Histology. Histology sections were stained with Masson's trichrome stain, in which the Weigert's iron hematoxylin stains the nuclei in black, the Biebrich scarlet-acid fuchsin stains the cytoplasm and muscle fibers in red, and the aniline blue stains the collagen in blue. The amount of collagen was calculated using the software Visiopharm version 3.2.8.0 (Visiopharm); collagen content is represented as a mean of the % of blue staining on three representative pictures of each slide. Images were acquired using Olympus DP71 U-PMTVC microscope digital camera (Olympus Corporation) connected to an Olympus BX60 light microscope.

The same monoclonal antibody employed in the α-SMA assay, which was used for tissue supernatants, was used in immunohistochemistry on histology sections. The α-SMA monoclonal antibody (NB552–2A11) was raised at Nordic Bioscience against the sequence 3′Ac-EEEDSTALV,[11] representing the acetylated N-terminal end of α-SMA. The specificity of the antibody was tested by incubating it in ELISA with the peptide it was raised against, the peptide elongated of one amino acid at the N-terminal end, and a non-sense peptide. Only the specific peptide could inhibit the signal in the competitive ELISA. The immunohistochemistry experiment was performed as follows: paraffin kidney sections were melted at 60 °C for 1 hour and were subsequently deparaffinized in toluene (2 × 5 minutes) and then rinsed in 99% ethanol (2 × 3 minutes). Peroxidases were blocked with 1.05% H_2O_2 in 99% ethanol (20 minutes), and the sections were rehydrated in 96% and then in 70% ethanol (2 × 3 minutes) and rinsed in tap water. The sections were incubated in citrate buffer (10 mM citric acid, 0.05% Tween 20, pH 6.0) for antigen retrieval (overnight). After a washing step in 0.1% Triton X-100 (2 × 5 minutes), the primary antibody NB552–2A11 (2.6 µg/mL Ab in Tris buffer pH 8.0) or a polyclonal mouse IgG Ab (Jackson ImmunoResearch)

Table 1. Markers measured in the supernatant of PCKS cultures.

MARKER	TARGET	MEASURES	REFERENCE
α-SMA	Acetylated N-terminal of α-smooth muscle actin	Marker for activated fibroblasts	(unpublished)
P1NP	N-terminal pro-peptide of collagen type I	Formation of collagen type I	25
C1M	MMP-generated collagen type I fragment	Degradation of collagen type I	26
C3M	MMP-generated collagen type III fragment	Degradation of collagen type III	27

as a negative control was added on the sections and incubated for 2 hours at room temperature. After a washing step in 0.1% Triton X-100 (2 × 5 minutes), the sections were incubated with super enhancer (Super Sensitive™* Polymer-HRP Detection System, BioGenex) for 20 minutes, washed in 0.1% Triton X-100 (2 × 5 minutes) and incubated with SS label polymer HRP (Super Sensitive™* Polymer-HRP Detection System, BioGenex) for 30 minutes. After a washing step in 0.1% Triton X-100 (2 × 5 minutes), the sections were incubated with DAP+ substrate (Dako) for 8–10 minutes, rinsed in tap water for 10 minutes, and counterstained in Mayer's hematoxylin for 1 minute. After a final rinse in tap water, the sections were mounted and observed under light microscopy.

Biomarker measurement. Markers for ECM turnover were measured in the supernatants of *ex vivo* cultures using competitive ELISAs previously developed at Nordic Bioscience. The list of measured markers and the corresponding references can be found in Table 1.

Active and total amount of transforming growth factor (TGF)-β was assessed using a commercial ELISA developed by BioLegend (Cat. 437707 and Cat. 436707).

Statistical analysis. All results are presented as mean ± standard error of the mean (SEM). The statistical differences between groups were calculated by the Wilcoxon test (paired nonparametric *t*-test), the Mann–Whitney test (unpaired nonparametric *t*-test), or the parametric paired and nonpaired *t*-test.

Results

One rat (#4) died immediately after UUO surgery, the other rats did not show any sign of distress until termination. The obstructed kidneys from UUO-operated animals were bigger than both the contralateral (left) kidney and the kidneys of the sham-operated animals (Fig. 1A).

The PCKS were cultured for five days. The UUO operation did not affect the viability of cultures, as shown in Figure 1B. The viability of the kidneys from UUO-operated animals (both the fibrotic right kidney and the contralateral kidney) decreased after five days of culturing compared with the first day of culture of only 45%, while kidneys from sham-operated rats had a decrease in viability of 60%. Cultures from the UUO-affected kidneys presented the highest levels of active TGF-β (Fig. 1C) in the supernatant.

Among the measured markers, P1NP (formation of collagen type I), C1M (MMP-mediated degradation of collagen type I), and C3M (MMP-mediated degradation of collagen type III) were markedly more elevated in cultures from obstructed kidneys than from both the contralateral kidney and the kidneys from sham-operated animals (Figs. 2A–C). Specifically, P1NP levels were sixfold increased, C1M was threefold increased, and C3M was fivefold increased in cultures from fibrotic kidneys. C1M was the only marker showing increased levels in the contralateral kidney of UUO-operated animals compared with the kidneys of the sham-operated animals. α-SMA was mostly undetectable in supernatants from nonfibrotic kidneys, while it was up to 13-fold more elevated in the supernatants of UUO-obstructed kidneys (Fig. 2D). The variation in the UUO right kidney group is quite large

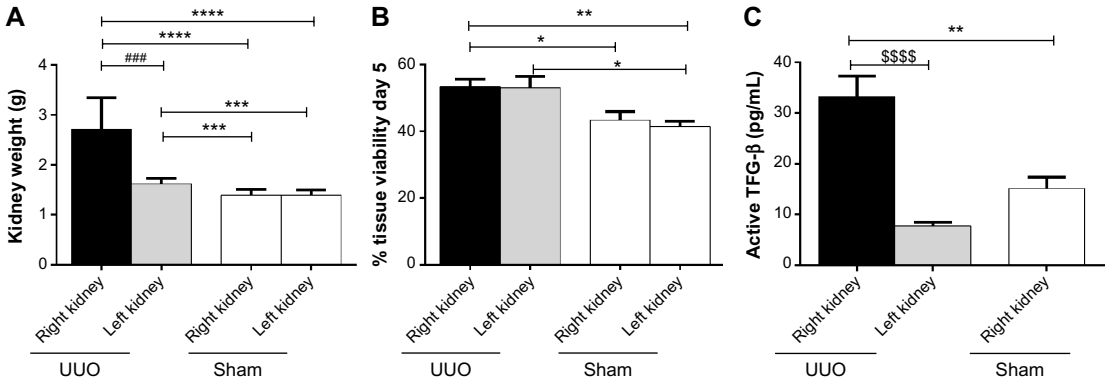

Figure 1. (**A**) Weight of excised kidneys at termination. The higher weight of obstructed kidneys was due to both enlargement of the kidney and the presence of excessive accumulated liquid in the tissue. (**B**) Tissue viability of PCKSs after 5 days of culture (% AlamarBlue® fluorescence compared with day 0). (**C**) Levels of active TGF-β in PCKS from UUO right and left kidneys and control right kidneys. Statistical difference calculated with parametric *t*-test (*$P < 0.05$; **$P < 0.01$; ****$P < 0.0001$), paired *t*-test (###$P < 0.001$), or Wilcoxon test ($$$$$P < 0.0001$).

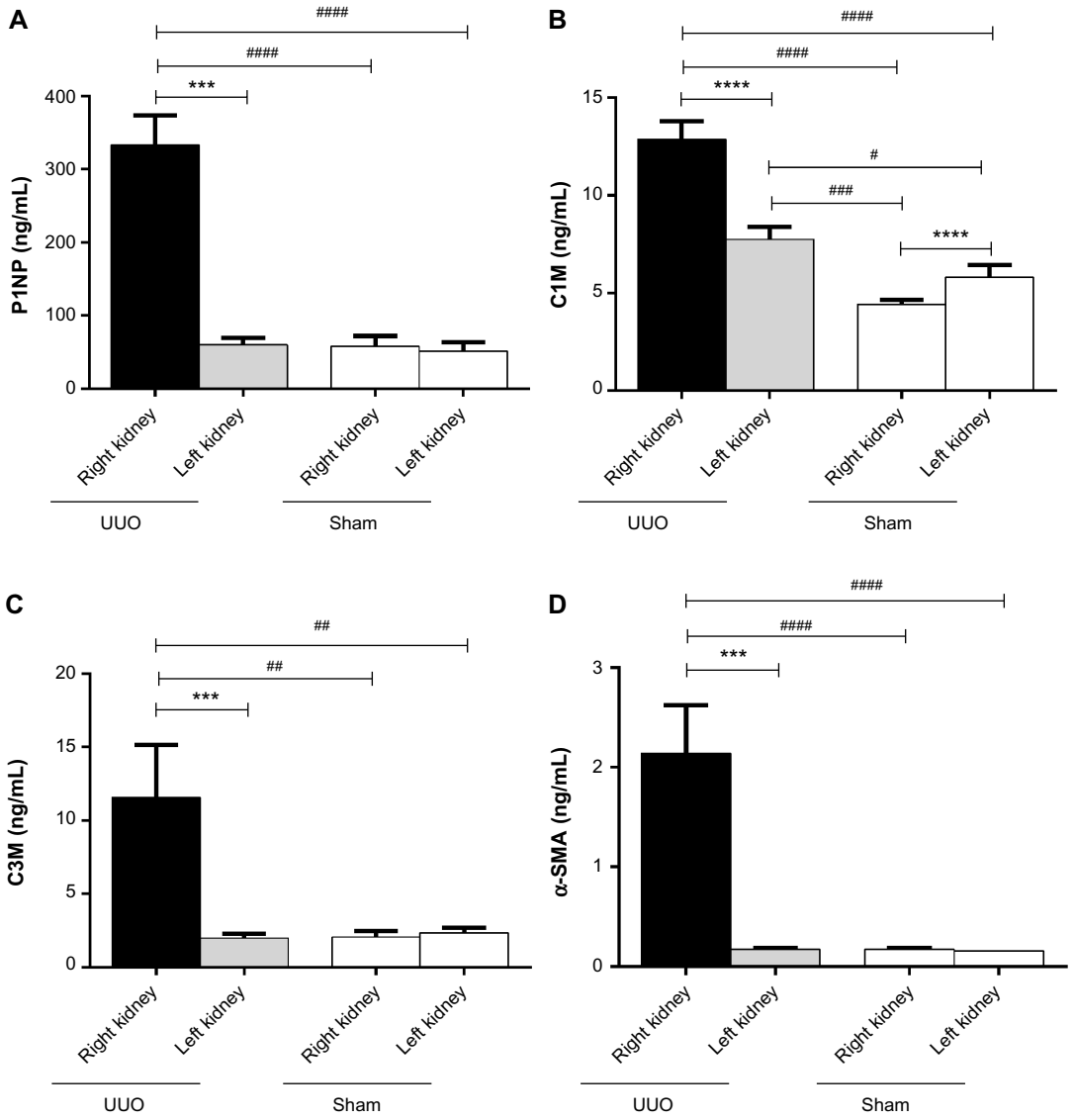

Figure 2. Concentration of ECM remodeling markers in supernatants of PCKS. Levels of P1NP (formation of collagen type I) (**A**), C1M (MMP-mediated degradation of collagen type I) (**B**), C3M (MMP-mediated degradation of collagen type III) (**C**), and α-SMA (**D**) in PCKS from UUO-operated animals (right kidney: obstructed kidney; left kidney: contralateral kidney) and control sham-operated animals (sham).
Notes: Statistical difference calculated with Wilcoxon test (***$P < 0.001$) or Mann–Whitney test (##$P < 0.01$; ####$P < 0.0001$). Data presented as mean ± SEM.

for all markers. Therefore, the levels of the markers in the individual animals were expressed as a percentage of the levels of the marker found in slices from the obstructed kidney as compared with slices from the contralateral kidney (Fig. 3). Animals that presented a mild increase in the relative amount of the markers also presented mild levels of fibrosis in histology (Figs. 3B, #1, #8, and #15), while animals presenting the highest differences in the markers from the obstructed and the contralateral kidney presented advanced fibrosis in histology, with destruction of the parenchyma and effacement of glomeruli (Figs. 3B, #7 and #11). The different patterns of soluble biomarkers released from the cultures of different animals reflect the variability in fibrosis development in different animals. In fact, the levels of P1NP, C3M, and α-SMA in the supernatants correlate with the levels of fibrosis in the tissue, described as % of collagen deposition (Spearman's $r = 0.78$, $P = 0.0004$; $r = 0.57$, $P = 0.02$; and $r = 0.81$, $P = 0.0002$, respectively; Fig. 4).

The immunohistochemical staining of α-SMA in paraffinized tissue confirmed what was shown by the soluble markers of fibrosis. Stronger staining, representing high presence of activated fibroblasts, was present in sections from the right kidney of animals that developed fibrosis and colocalized with collagen deposition as observed by Masson's trichrome staining (Fig. 5).

Discussion

PCTSs have been known and used for at least three decades as a tool to study organ toxicity after exposure to xenobiotics, such as pollutant and drugs.[11–14] PCTSs of liver are the

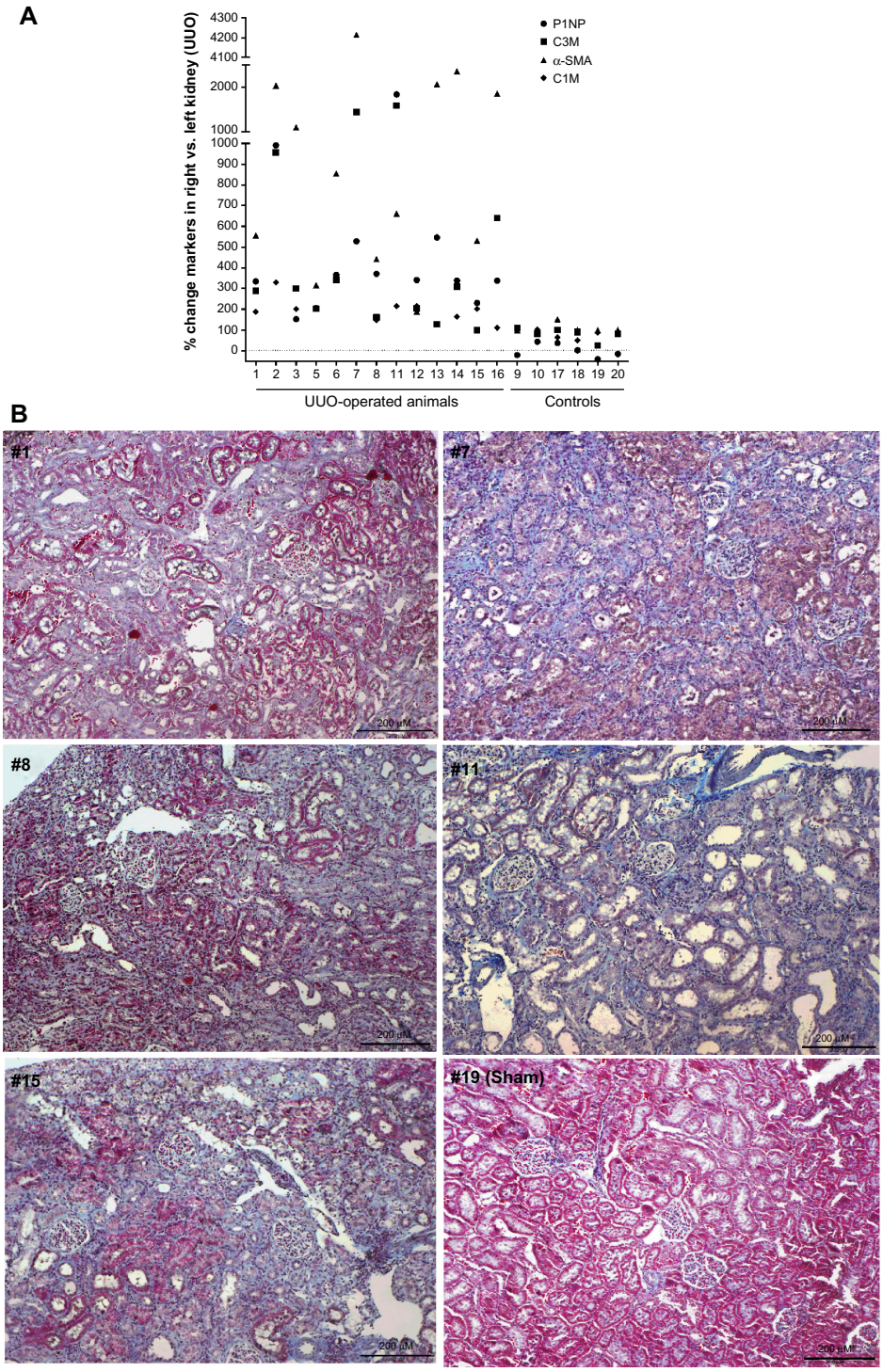

Figure 3. (**A**) % level of markers in supernatant of PCKS from the right kidney (the obstructed one in UUO-operated animal) compared with the left kidney in individual animals. (**B**) Representative sections of right kidneys from five UUO-operated animals (#1, #7, #8, #11, and #15) and a sham-operated animal (#19), stained with Masson's trichrome staining.

most routinely studied, but other organs, such as the lungs, intestines, and kidneys, have also been used to develop *ex vivo* models to observe physiological and pathological events in an environment that resembled the *in vivo* conditions better than single-cell culture or even co-cultures.[7] The use of PCTS to study the mechanisms of fibrosis and the efficacy of antifibrotic treatments is more recent.[8] However, most of these models use healthy tissues from rats or mice and stimulate them with TGF-β1 to induce a fibrogenic response.[15–17] In a recent study, the use of PCTS from human kidneys has been proposed to study the mechanisms of fibrosis.[18] However also in this experimental approach, fibrosis is induced in already cultured slices by means of TGF-β stimulation. In our experiment, we used fibrotic kidneys, in order to improve translational science,

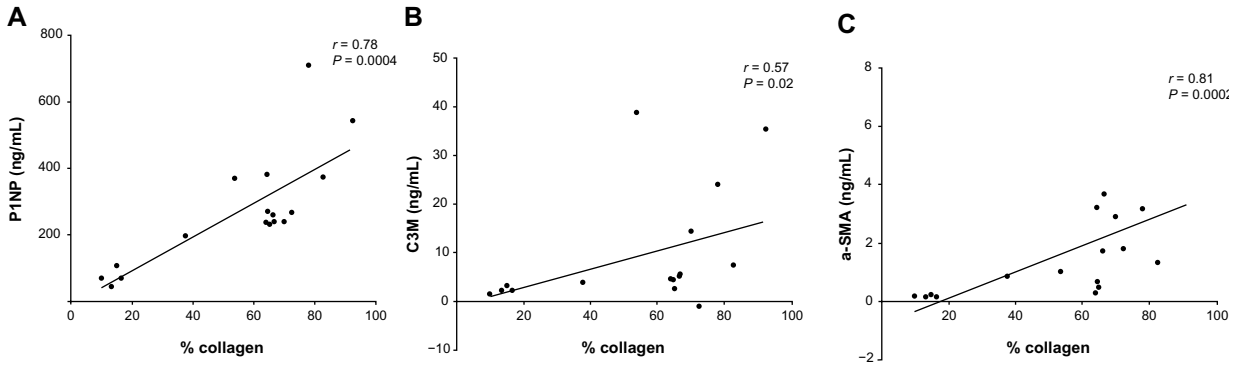

Figure 4. Correlation plot of degree of fibrosis (evaluated as the mean of the % of blue staining on three representative pictures of each slide stained with Masson's trichrome staining) in the right kidney of different animals with marker levels in tissue supernatant.

since fibrotic organs present a more altered metabolic profile compared with healthy ones.[19] We have chosen the UUO surgery to induce kidney fibrosis in 12-week-old rats. UUO is a widely used model for studying renal interstitial fibrosis,[20] and it resembles the pathophysiology of human chronic obstructive nephropathy in an accelerated manner.[21] Furthermore, this model presents the advantage of the presence of the contralateral kidney, which can act as internal negative control; in this case, we observed a possible compensatory effect of the left kidney due to the lack of function of the obstructed kidney.[22] This might partially explain the higher survival rate of slices from the contralateral kidneys of UUO-operated animals compared with slices from the corresponding left kidney of sham-operated animals, as well as the slightly increased weight of the organ. Moreover, it is possible to observe higher levels of the markers C1M released from the contralateral kidney compared with both kidneys from the sham-operated animals. Despite this is the only marker showing this trend, a high level of collagen type I remodeling can reflect an initial fibrogenic process starting in the contralateral kidney. This is not the first time that kidneys from UUO-operated animals have been used in an *ex vivo* setting.[10] However, it is the first time that a standardized PCKS experiment using thin slices (250 µm vs 1.5 mm)[10] cultured for five days has been performed with the aim of observing the dynamics of ECM remodeling in fibrotic kidneys. The novelty of our approach lies not only in the use of fibrotic kidneys but also in the investigation of soluble fragments of ECM proteins, which reflect the dynamic process of turnover, rather than observing ECM protein translation by mRNA quantification or accumulation in the tissue by histology. In this study, we have observed a 6-fold increase of a soluble marker of collagen type I formation and a 3-fold increase of a marker of collagen type I degradation, a 5-fold increase of a marker of degradation of collagen type III, and a 13-fold increase of α-SMA release in the supernatant from obstructed kidneys from UUO-operated rats compared with both the not affected kidney and the kidneys from sham-operated rats. The increase in α-SMA released into the supernatants was reflected by the levels of α-SMA staining in the tissue of fibrotic animals. α-SMA is a marker for activated fibroblasts, and herein, we demonstrate that our newly developed assay recognizing the acetylated

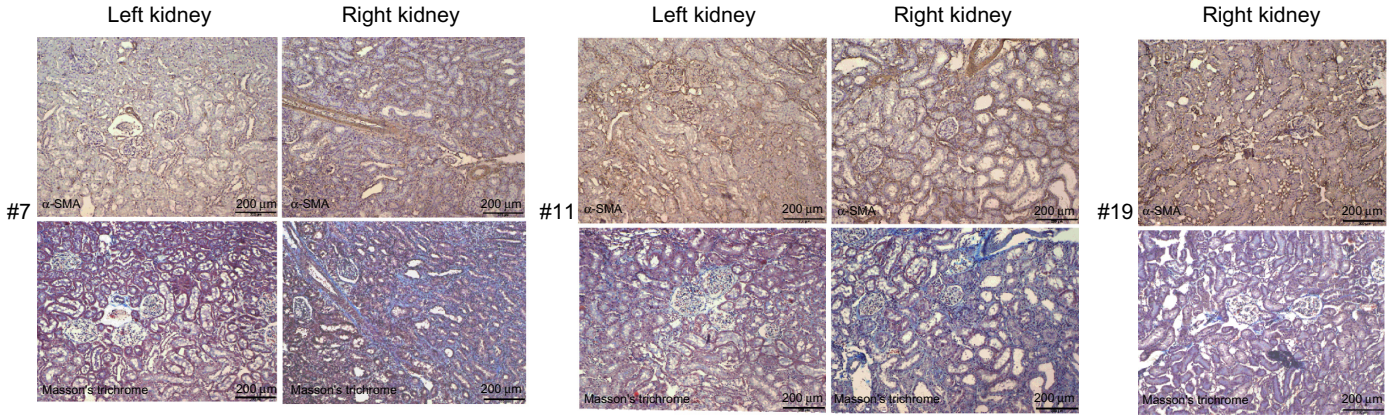

Figure 5. α-SMA immunohistochemistry on two representative UUO-operated animals (#7 and #11) and a representative sham-operated animal (#19). The left kidney is the contralateral kidney. The α-SMA staining in the operated right kidney colocalize with the collagen deposition in the Masson's trichrome staining, in blue.

version of the molecule can be used in solution to quantify the levels of fibrosis in a tissue. The increased levels of P1NP, C1M, and C3M in supernatants of UUO PCKS suggest an increase in both formation and degradation of the interstitial collagens in the process of tubulointerstitial fibrosis. Collagen type I and III are the most abundant interstitial collagens in kidneys. They colocalize in the renal tubular interstitium, and therefore, their remodeling is strongly interconnected, as demonstrated by the similar increase observed in the degradation markers C1M and C3M in UUO-operated kidneys compared with either the contralateral kidneys or the kidneys from the sham-operated animals.

The increased presence of the profibrotic mediator TFG-β in its active form in PCTS from the affected kidneys could be an explanation for the differences in the fibrosis markers. This is in agreement with previous results obtained in other rat models of tubulointerstitial fibrosis, where markers for collagen type I and III degradation were markedly higher in the urine of disease-affected animals compared with healthy controls.[23] This model could constitute the bridge to link the levels of the markers in biological fluid to the tissue of origin. Markers of ECM remodeling have also been measured in human urine in patients with IgA nephropathy,[24] showing a different pattern for the C3M assay (describing collagen type III degradation). C3M was decreased in advanced stages of the disease, which are characterized by higher extent of fibrosis. On the contrary, a marker of collagen type III formation (Pro-C3) was increased, showing a prevalence of collagen formation over degradation in the presence of advanced kidney fibrosis. These results should be coupled with results from PCTS performed on fibrotic kidneys from IgA nephropathy patients to confirm the renal origin of the markers.

The variation in the levels of the markers and in the weight of the kidneys in the UUO-operated group can be explained by the different degrees of fibrosis developed by the animals following the ligation of the ureter. The UUO model is known to have a high degree of reproducibility[20]; however individual susceptibility to the surgery and the variation introduced by the operator during the surgery must be taken into account. We have demonstrated that soluble markers of ECM remodeling were able to differentiate animals that developed different degrees of fibrosis and that the levels of collagen type I formation and type III degradation and α-SMA release correlated with the levels of collagen deposition in the kidneys, which was evaluated by histology. The high variability of the used model of CKD is an intrinsic limitation of this work: despite this, the PCTS model that we presented possesses high potential for the evaluation of the ECM remodeling occurring during fibrosis and possibly its modulation by means of antifibrotic drugs. The reproducibility of the UUO model needs to be ameliorated to reduce interindividual variability. Alternatively, another model of CKD warranting a better uniformity can be used as source of kidneys for the PCKS model.

Conclusions

In this work, we introduced the use of soluble markers for ECM remodeling in precision-cut slices of fibrotic kidneys, which could be used as a tool to monitor the efficacy of antifibrotic drugs *ex vivo* in real time. Moreover, such markers can be used in translational science, since the assays target epitopes that are conserved in different rodent species and human beings, and in addition, the same markers can be measured in biological fluids, such as serum and urine, allowing for a direct correlation between the protein fragments found in circulation or secreted in the urine, and those coming from the diseased tissue.

Author Contributions

Conceived and designed the experiments: FG, ZSK. Analyzed the data: ZSK, SHN. Wrote the first draft of the manuscript: FG. Contributed to the writing of the manuscript: ZSK, SHN, MAK. Agree with manuscript results and conclusions: FG, MAK. Jointly developed the structure and arguments for the paper: FG, MAK. Made critical revisions and approved final version: MAK. All authors reviewed and approved of the final manuscript.

REFERENCES

1. Wynn TA. Cellular and molecular mechanisms of fibrosis. *J Pathol*. 2008;214:199–210.
2. Boor P, Ostendorf T, Floege J. Renal fibrosis: novel insights into mechanisms and therapeutic targets. *Nat Rev Nephrol*. 2010;6:643–56.
3. Zeisberg M, Neilson EG. Mechanisms of tubulointerstitial fibrosis. *J Am Soc Nephrol*. 2010;21:1819–34.
4. Flamant M, Placier S, Rodenas A, et al. Discoidin domain receptor 1 null mice are protected against hypertension-induced renal disease. *J Am Soc Nephrol*. 2006;17:3374–81.
5. Genovese F, Manresa AA, Leeming DJ, Karsdal MA, Boor P. The extracellular matrix in the kidney: a source of novel non-invasive biomarkers of kidney fibrosis? *Fibrogenesis Tissue Repair*. 2014;7:4.
6. Karsdal MA, Nielsen MJ, Sand JM, et al. Extracellular matrix remodeling: the common denominator in connective tissue diseases. Possibilities for evaluation and current understanding of the matrix as more than a passive architecture, but a key player in tissue failure. *Assay Drug Dev Technol*. 2013;11:70–92.
7. Hansen NU, Genovese F, Leeming DJ, Karsdal MA. The importance of extracellular matrix for cell function and *in vivo* likeness. *Exp Mol Pathol*. 2015;98:286–94.
8. Westra IM, Pham BT, Groothuis GM, Olinga P. Evaluation of fibrosis in precision-cut tissue slices. *Xenobiotica*. 2013;43:98–112.
9. De Graaf I, Olinga P, De Jager MH, et al. Preparation and incubation of precision-cut liver and intestinal slices for application in drug metabolism and toxicity studies. *Nat Protoc*. 2010;5:1540–51.
10. Nagae T, Mori K, Mukoyama M, et al. Adrenomedullin inhibits connective tissue growth factor expression, extracellular signal-regulated kinase activation and renal fibrosis. *Kidney Int*. 2008;74:70–80.
11. Parrish AR, Gandolfi AJ, Brendel K. Precision-cut tissue slices: applications in pharmacology and toxicology. *Life Sci*. 1995;57:1887–901.
12. De Kanter R, Monshouwer M, Meijer DK, Groothuis GM. Precision-cut organ slices as a tool to study toxicity and metabolism of xenobiotics with special reference to non-hepatic tissues. *Curr Drug Metab*. 2002;3:39–59.
13. Obatomi DK, Thanh NT, Brant S, Bach PH. The toxic mechanism and metabolic effects of atractyloside in precision-cut pig kidney and liver slices. *Arch Toxicol*. 1998;72:524–30.
14. Phelps JS, Gandolfi AJ, Brendel K, Dorr RT. Cisplatin nephrotoxicity: in vitro studies with precision-cut rabbit renal cortical slices. *Toxicol Appl Pharmacol*. 1987;90:501–12.
15. Pham BT, van Haaften WT, Oosterhuis D, Nieken J, De Graaf I, Olinga P. Precision-cut rat, mouse, and human intestinal slices as novel models for the early-onset of intestinal fibrosis. *Physiol Rep*. 2015;3:e12323.
16. Poosti F, Pham BT, Oosterhuis D, et al. Precision-cut kidney slices (PCKS) to study development of renal fibrosis and efficacy of drug targeting ex vivo. *Dis Model Mech*. 2015;8(10):1227–36.

17. Westra IM, Oosterhuis D, Groothuis GM, Olinga P. Precision-cut liver slices as a model for the early onset of liver fibrosis to test antifibrotic drugs. *Toxicol Appl Pharmacol*. 2014;274:328–38.
18. Stribos EGD, Luangmonkong T, Leliveld AM, et al. Precision-cut human kidney slices as a model to elucidate the process of renal fibrosis. *Translational Research: the Journal of Laboratory and Clinical Medicine*. 2016;170:8–16.
19. Veidal SS, Nielsen MJ, Leeming DJ, Karsdal MA. Phosphodiesterase inhibition mediates matrix metalloproteinase activity and the level of collagen degradation fragments in a liver fibrosis ex vivo rat model. *BMC Res Notes*. 2012;5:686.
20. Chevalier RL, Forbes MS, Thornhill BA. Ureteral obstruction as a model of renal interstitial fibrosis and obstructive nephropathy. *Kidney Int*. 2009;75:1145–52.
21. Hewitson TD. Renal tubulointerstitial fibrosis: common but never simple. *Am J Physiol Renal Physiol*. 2009;296:F1239–44.
22. Katz AI. Renal function immediately after contralateral nephrectomy: relation to the mechanism of compensatory kidney growth. *Yale J Biol Med*. 1970;43:164–72.
23. Papasotiriou M, Genovese F, Klinkhammer BM, et al. Serum and urine markers of collagen degradation reflect renal fibrosis in experimental kidney diseases. *Nephrol Dial Transplant*. 2015;30:1112–21.
24. Genovese F, Boor P, Papasotiriou M, Leeming DJ, Karsdal MA, Floege J. Turnover of type III collagen reflects disease severity and is associated with progression and microinflammation in patients with IgA nephropathy. *Nephrol Dial Transplant*. 2015;31(3):472–9.
25. Leeming DJ, Larsen DV, Zhang C, et al. Enzyme-linked immunosorbent serum assays (ELISAs) for rat and human N-terminal pro-peptide of collagen type I (PINP) – assessment of corresponding epitopes. *Clin Biochem*. 2010;43:1249–56.
26. Leeming D, He Y, Veidal S, et al. A novel marker for assessment of liver matrix remodeling: an enzyme-linked immunosorbent assay (ELISA) detecting a MMP generated type I collagen neo-epitope (C1M). *Biomarkers*. 2011;16:616–28.
27. Barascuk N, Veidal SS, Larsen L, et al. A novel assay for extracellular matrix remodeling associated with liver fibrosis: an enzyme-linked immunosorbent assay (ELISA) for a MMP-9 proteolytically revealed neo-epitope of type III collagen. *Clin Biochem*. 2010;43:899–904.